

Stark-broadening calculations of the Lyman- α line in a turbulent plasma*

C. Deutsch

Laboratoire de Physique des Plasmas, Université Paris XI, 91-Orsay, France

G. Bekefi

*Department of Physics and Research Laboratory of Electronics, Massachusetts Institute of Technology,
Cambridge, Massachusetts 02139*

(Received 7 January 1976)

The low-frequency microfield arising from homogeneous, anisotropic, partially developed turbulence is represented by a Gaussian distribution, and is introduced into a generalized computation of the hydrogen Ly α line. The electrons are taken to be thermal, and they provide their usual impact broadening in the line center, while their effect is neglected in the wings. Analytical approximations, valid either in the line center or in the wings, are obtained for the polarized profiles emitted both parallel and perpendicular to the turbulence axis. This axis is simulated by a fictitious magnetic field \vec{B} which is allowed to vanish at the end of the calculations. The line profiles are characterized by the anisotropy parameter $\eta^2 = 2\langle E_{\parallel}^2 \rangle / \langle E_{\perp}^2 \rangle$ where $\langle E_{\parallel}^2 \rangle$ and $\langle E_{\perp}^2 \rangle$ are the mean square electric field components parallel and perpendicular to the turbulence axis of the microfield, respectively.

I. INTRODUCTION

In a turbulent plasma the low-frequency microfield distribution (ionic field) does not retain its usual thermal Holtzmark-like form.¹ There is an increasing body of fairly convincing evidence that turbulence may be considered as a vectorial superposition of a very large number of statistically independent fluctuations, so that the central limit theorem (CLT) of probability theory may be invoked; accordingly, the components of the resulting electric field have a Gaussian distribution. This is confirmed by observations of the hydrogenic 2^1P-4^1D 4921- \AA He I line broadened by the highly nonthermal plasma produced in a θ pinch;² it also agrees with a recent determination of the strong turbulence spectrum³ in a beam-plasma experiment. On the theoretical side, several speculations about the turbulence spectrum have reached similar conclusions. The instability spectrum observed in certain types of fusion devices led some authors⁴ to simulate their corresponding low-frequency probability distribution with a superposition of Rayleigh (Gaussian) distributions, as is explained in Sec. II. Self-consistent treatments based either upon the quasilinear theory of wave-particle-generated weak turbulence,⁵ or on the evaluation of the enhancement of the collective contributions to the microfield, likewise reproduce the above-mentioned Gaussian behavior in momentum as well as in configuration space.^{6,7}

In this paper we shall pay particular attention to the low-frequency microfield produced by ions assumed to be nearly static. In this manner we simulate the low-frequency turbulent spectrum pro-

duced, say, by an ion-acoustic wave³ or other related mechanisms. The corresponding distribution is then folded with the usual impact electron profile in order to simulate in a realistic way the influence of turbulent Stark broadening on hydrogen lines. The usefulness and the credibility of such an approach has been previously emphasized⁸ in connection with the quasistatic broadening of the hydrogenic 4471- \AA He I line in the presence of fully developed isotropic turbulence represented by a three-dimensional Gaussian distribution, taken as a working example.

The present paper is organized as follows: In Sec. II the anisotropic Sholin-Oks distribution⁴ is used to model the low-frequency turbulent plasma-atom interaction. The nonthermal energy fed into the ions is taken to be large enough to allow one to neglect the usual thermal probability distribution.¹ Moreover, in order to define unambiguously the turbulence symmetry axis, we suppose it to be along a small static magnetic field \vec{B} , playing the role of a Tauberian parameter which is allowed to go to zero at the end of the calculations. As a by-product, this approach enables one to retain any real combined Stark and Zeeman effect related to nonzero B values, arising from turbulent heating,⁹ for instance. We present in Sec. III the generalized impact formalism in the presence of a static magnetic field,^{10,11} and derive in Sec. IV the $B \rightarrow 0$ analytical approximations valid in the center and in the line wings, for the polarized intensities emitted, respectively, parallel and perpendicular to the turbulence axis specified by the vector \vec{B} . The corresponding numerical analysis is then displayed in Sec. V, with the anisotropy factor $\eta^2 = 2\langle E_{\parallel}^2 \rangle / \langle E_{\perp}^2 \rangle$ taken as a running parameter.

II. TURBULENT PLASMA-ATOM INTERACTION

We have already presented⁸ a quasistatic analysis of the 4471-Å He I line broadened by ions in a strongly turbulent plasma with the three-dimensional Gaussian microfield distribution

$$W(E) dE = 4\pi(1/2\pi\sigma)^{3/2} E^2 e^{-E^2/2\sigma} dE, \quad (2.1)$$

and also in a weakly turbulent plasma with the one-dimensional Gaussian

$$W(E) dE = (1/2\pi\sigma)^{1/2} e^{-E^2/2\sigma} dE. \quad (2.2)$$

In both cases, we noted the characteristic Gaussian fall-off in the wings transmitted by the quasi-linear Stark effect of the hydrogenic He I lines. However, the one-dimensional calculation displayed some numerical discontinuities, calling clearly for a smoothing of the final profile through the inclusion of the usual thermal electron contribution. Also, and even more importantly, experimental observation⁴ suggests that the anisotropy brought about by the partially developed turbulence induced by growing waves propagating primarily along a given direction has to be taken into account in the static microfield distribution. Therefore in

order to retain the physical complexity of the turbulent spectrum with waves traveling also perpendicularly to the above-mentioned turbulent axis (and depicted by a fictitious Tauberian magnetic field \vec{B}) we shall follow Sholin and Oks⁴ and specify the low-frequency microfield as a superposition of a one-dimensional noise spectrum with a wave vector along $\vec{B} \parallel \vec{o}_z$ and a two-dimensional spectrum with a wave vector in the perpendicular plane. Each of these two spectra represents the result of the compounding of a very large number of oscillations with random phases. The amplitude distribution in each of them may be expressed by the corresponding Rayleigh distributions,

$$W_1(\vec{E}_{\parallel}) d\vec{E}_{\parallel} = (2\pi\langle E_{\parallel}^2 \rangle)^{-1/2} \exp(-E_{\parallel}^2/2\langle E_{\parallel}^2 \rangle) dE_{\parallel}, \quad (2.3a)$$

$$W_2(\vec{E}_{\perp}) d\vec{E}_{\perp} = 2(\langle E_{\perp}^2 \rangle)^{-1} \exp(-E_{\perp}^2/\langle E_{\perp}^2 \rangle) E_{\perp} dE_{\perp}, \quad (2.3b)$$

with the average fields taken to be much larger than the Holtmark contribution $E_0 = 2.603eN^{2/3}$ given in terms of the charged-particles density $N = N_e = N_i$. The distribution of the total turbulent electric field $\vec{E} = \vec{E}_{\parallel} + \vec{E}_{\perp}$ may then be written

$$\begin{aligned} W(E, \cos\theta) dE d\cos\theta &= \int d\vec{E}_{\parallel} \int d\vec{E}_{\perp} W_1(\vec{E}_{\parallel}) W_2(\vec{E}_{\perp}) \delta(\vec{E} - \vec{E}_{\parallel} - \vec{E}_{\perp}) dE d\cos\theta \\ &= \left(\frac{2}{\pi\langle E_{\parallel}^2 \rangle} \right)^{1/2} \frac{E^2}{\langle E_{\perp}^2 \rangle} \exp \left[-\frac{E^2}{E_{\perp}^2} - \cos^2\theta \left(\frac{E^2}{2\langle E_{\parallel}^2 \rangle} - \frac{E^2}{\langle E_{\perp}^2 \rangle} \right) \right] dE d\cos\theta. \end{aligned} \quad (2.4)$$

The directional diagram corresponding to Eq. (2.4) is an ellipsoid of revolution with the axis \vec{o}_z . As the degree of anisotropy $\eta^2 = 2\langle E_{\parallel}^2 \rangle / \langle E_{\perp}^2 \rangle$ increases steadily from 0 to ∞ , the ellipsoid changes its form from an oblate "lens" to a very extended "sausage," taking the form of a sphere for $\eta^2 = 1$. In the following analysis the magnetic field B will be taken to be sufficiently weak such that the electron Larmor frequency be small compared with the electron plasma frequency. That is,

$$(n-1)eB/2m_e c \ll \omega_{pe}, \quad (2.5)$$

which for the hydrogen Lyman- α line imposes the inequality $220B(\text{G}) N^{-1/2}(\text{cm}^{-3}) \ll 1$.

III. LYMAN- α PROFILES

A. General formulation

Using the anisotropic microfield distribution (2.4), we may now proceed along the lines of the combined Stark and Zeeman calculations described elsewhere.^{10,11} However, we shall outline only the more significant features of this formalism, relevant to the present work. Let us consider then the

emitted intensity polarized along the unit vector \vec{e} :

$$I_{\vec{e}}(\omega) = \int d\vec{E} W(\vec{E}) I_{\vec{e}}(\omega, \vec{E}, \vec{B}), \quad (3.1)$$

where $I_{\vec{e}}(\omega, \vec{E}, \vec{B})$ is expressed in terms of the standard generalized impact profile as

$$\begin{aligned} I_{\vec{e}}(\omega, \vec{E}, \vec{B}) &= \pi^{-1} \text{Re} \sum_{ijk} \langle \psi_i | \vec{e} \cdot \vec{r} | \phi_j \rangle \langle \phi_j | \vec{e} \cdot \vec{r} | \psi_k \rangle \\ &\quad \times \langle \psi_i | [i(\Delta\omega - \Delta\omega_{ij}) - \Phi^{(n)}]^{-1} | \psi_k \rangle, \end{aligned} \quad (3.2)$$

with $\Delta\omega = \omega - \omega_0$. The quantity $\omega_0 = (E_0^{(n)} - E_0^{(n')})/\hbar^{-1}$ is the unperturbed energy, while

$$\Delta\omega_{ij} = [\langle \psi_i | (H - E_0^{(n)}) | \psi_i \rangle - \langle \phi_j | (H - E_0^{(n')}) | \phi_j \rangle] \hbar^{-1}$$

is the energy expressed in terms of the upper and lower statically perturbed levels associated with the wave functions ψ_i and ϕ_j . With the low-frequency turbulence concentrated in the ionic component, we then retain the usual thermal electron impact broadening in the term Φ and write it in the standard Griem-Kolb-Shen operator formalism¹² as

($n' = 1$). In the Ly α case, matters simplify considerably with $p = s$ and $p = q$, respectively, while

$$\langle nl'm' | (\vec{r} \cdot \vec{r}/a_0^2) | nlm \rangle = \frac{9}{4} n^2 [n^2 - (l^2 + l + 1)] \delta_{ll'} \delta_{mm'}. \quad (3.12)$$

The final profile for the emitted light polarized along \vec{e} then reads

$$S_{\vec{e}_2}(\alpha) = \int d\vec{E} W(\vec{E}) S_{\vec{e}}(\alpha, A, \gamma). \quad (3.13)$$

$$S_{\vec{e}}(\alpha) = \pi \int_0^\infty dE \int_{-1}^{+1} d\gamma \{ \cos^2 \theta_0 [S_{\vec{e}_x}(\alpha, A, \gamma) + S_{\vec{e}_y}(\alpha, A, \gamma)] + 2 \sin^2 \theta_0 S_{\vec{e}_z}(\alpha, A, \gamma) \} W(E, \gamma), \quad (3.15)$$

with $\vec{e}_2 = (-\cos \theta_0 \cos \phi, \cos \theta_0 \sin \phi, \sin \theta_0)$ (see Fig. 1). Finally, an averaging over the azimuthal angle ϕ is performed with the aid of the identities

$$\int_0^{2\pi} d\phi \cos^2 \phi = \int_0^{2\pi} d\phi \sin^2 \phi = \pi,$$

etc.

We now assume that the observations of the line shapes are performed without a polarizer, and with that in mind, we introduce the two normalized intensities S_{\parallel} and S_{\perp} ,

$$\begin{aligned} S_{\theta_0}(\alpha) &= \frac{1}{2} [S_{\vec{e}_1}(\alpha) + S_{\vec{e}_2}(\alpha)] \\ &= \cos^2 \theta_0 S_{\parallel}(\alpha) + \sin^2 \theta_0 S_{\perp}(\alpha), \end{aligned} \quad (3.16)$$

defined as

$$\begin{aligned} S_{\parallel}(\alpha) &= \pi \int_0^\infty dE \int_{-1}^{+1} d\gamma W(E, \gamma) \\ &\quad \times [S_{\vec{e}_x}(\alpha, A, \gamma) + S_{\vec{e}_y}(\alpha, A, \gamma)], \end{aligned} \quad (3.17)$$

$$\begin{vmatrix} -\xi & 3A(1-\gamma^2)^{1/2}/\sqrt{2} & 3A\gamma & -3A(1-\gamma^2)^{1/2}/\sqrt{2} \\ 3A(1-\gamma^2)^{1/2}/\sqrt{2} & -(\xi+1) & 0 & 0 \\ 3A\gamma & 0 & -\xi & 0 \\ -3A(1-\gamma^2)^{1/2}/\sqrt{2} & 0 & 0 & -(\xi-1) \end{vmatrix} \begin{vmatrix} a^1 \\ a^2 \\ a^3 \\ a^4 \end{vmatrix} = 0. \quad (3.19)$$

Then, solving the characteristic equation

$$\xi^4 - \xi^2(1+9A^2) + 9A^2\gamma^2 = 0 \quad (3.20)$$

for the eigenvalues yields

$$\xi = \epsilon_1 \left(\frac{1+9A^2}{2} \right)^{1/2} \left[1 - \epsilon_2 \left(1 - \frac{36A^2\gamma^2}{(1+9A^2)^2} \right)^{1/2} \right]^{1/2}, \quad (3.21)$$

$$\epsilon_1, \epsilon_2 = \pm 1,$$

together with

It will prove useful to specialize the analysis to two cases, namely,

$$\begin{aligned} S_{\vec{e}_1}(\alpha) &= \pi \int_0^\infty dE \int_{-1}^{+1} d\gamma [S_{\vec{e}_x}(\alpha, A, \gamma) \\ &\quad + S_{\vec{e}_y}(\alpha, A, \gamma)] W(E, \gamma), \end{aligned} \quad (3.14)$$

with $\vec{e}_1 = (\sin \phi, \cos \phi, 0)$, and

$$\begin{aligned} S_{\perp}(\alpha) &= \frac{\pi}{2} \int_0^\infty dE \int_{-1}^{+1} d\gamma W(E, \gamma) \\ &\quad \times [S_{\vec{e}_x}(\alpha, A, \gamma) + S_{\vec{e}_y}(\alpha, A, \gamma) \\ &\quad + 2S_{\vec{e}_z}(\alpha, A, \gamma)]. \end{aligned} \quad (3.18)$$

They are the intensities as observed parallel and perpendicular to \vec{B} , respectively. Equations (3.17) and (3.18) provide the basis for our anisotropic polarization-dependent analysis of turbulent Stark broadening, with the thermal electron impact contribution retained in the line center.

C. Static algebra

It remains to apply the above expression to the Ly α line, and to diagonalize Eq. (3.5) for the eigenvector components a , through the relationship

$$\begin{aligned} a^1 &= [(1-\xi^2)/2(1+9A^2-2\xi^2)]^{1/2}, \\ a^2 &= \frac{3}{2} A(1-\gamma^2)^{1/2}/(1+\xi) [(1-\xi^2)/(1+9A^2-2\xi^2)]^{1/2}, \\ a^3 &= (3A\gamma/\xi) [(1-\xi^2)/2(1+9A^2-2\xi^2)]^{1/2}, \\ a^4 &= \frac{3}{2} A(1-\gamma^2)^{1/2}/(1-\xi) [(1-\xi^2)/2(1+9A^2-2\xi^2)]^{1/2}. \end{aligned} \quad (3.22)$$

Note that $\sum_{i=1}^4 a^{i2} = 1$. As a consequence, the reduced collision operator $\Gamma^{(2)} = \vec{Q} \vec{r} \cdot \vec{r}/a_0^2$ may be given the matrix representation

$$\mathcal{G} \begin{pmatrix} 27 & 0 & 0 & 0 \\ 0 & 9 & 0 & 0 \\ 0 & 0 & 9 & 0 \\ 0 & 0 & 0 & 9 \end{pmatrix}, \quad (3.23)$$

with

$$\mathcal{G} = 7.212 \times 10^{-10} N_e^{1/3} (\text{cm}^{-3}) T_e^{-1/2} (^\circ\text{K}) \times \{13.76 - 0.5 \ln[N_e (\text{cm}^{-3}) / T_e (^\circ\text{K})]\}. \quad (3.24)$$

The anisotropic electron profiles then become

$$S_{\parallel}(\alpha, A, \gamma) = \frac{2}{\pi} \sum_{\epsilon=\pm 1} \left(\frac{9\mathcal{G}}{81\alpha^2 + (\alpha - K_\epsilon)^2} + \frac{9\mathcal{G}}{81\alpha^2 + (\alpha + K_\epsilon)^2} \right) \times \left(\frac{\epsilon(1 - 9A^2\gamma^2)}{[(1 + 9A^2)^2 - 36A^2\gamma^2]^{1/2} + 1} \right), \quad (3.25)$$

$$S_{\perp}(\alpha, A, \gamma) = \pi^{-1} \sum_{\epsilon=\pm 1} \left(\frac{9\mathcal{G}}{81\alpha^2 + (\alpha - K_\epsilon)^2} + \frac{9\mathcal{G}}{81\alpha^2 + (\alpha + K_\epsilon)^2} \right) \times \left(\frac{-\epsilon 9A^2(1 - \gamma^2)}{2[(1 + 9A^2)^2 - 36A^2\gamma^2]^{1/2} + 1} \right), \quad (3.26)$$

where

$$K_\epsilon = \frac{\lambda_0^2}{2\pi m_e c A_0} \left(\frac{1 + 9A^2}{2} \right)^{1/2} \times \left[1 + \epsilon \left(1 - \frac{36A^2\gamma^2}{(1 + 9A^2)^2} \right)^{1/2} \right]^{1/2}. \quad (3.27)$$

In accordance with the prescription given in Sec. I, we now set the Tauberian parameter equal to zero. Thus as $B \rightarrow 0$,

$$A = e a_0 \langle E_{\parallel, \perp}^2 \rangle^{1/2} / \hbar \omega_L \gg e a_0 E_0 / \hbar \omega_L \gg 1, \quad (3.28)$$

with the result that

$$S_{\parallel}(\alpha, A, \gamma) \approx \frac{2}{\pi} \left[2(1 + \gamma^2) \frac{9\mathcal{G}}{81\alpha^2 + \alpha^2} + (1 - \gamma^2) \left(\frac{9\mathcal{G}}{81\alpha^2 + (\alpha - \alpha_S)^2} + \frac{9\mathcal{G}}{81\alpha^2 + (\alpha + \alpha_S)^2} \right) \right], \quad (3.29)$$

$$S_{\perp}(\alpha, A, \gamma) \approx \pi^{-1} \left[\frac{(3 - \gamma^2) 9\mathcal{G}}{81\alpha^2 + \alpha^2} + \left(\frac{1 + \gamma^2}{2} \right) \left(\frac{9\mathcal{G}}{81\alpha^2 + (\alpha - \alpha_S)^2} + \frac{9\mathcal{G}}{81\alpha^2 + (\alpha + \alpha_S)^2} \right) \right]. \quad (3.30)$$

Here $\alpha_S = (3\beta \hbar \lambda_0^2) / (2\pi m_e c)$. Note that the first term

on the right-hand side of the last two equations represents the contribution to the central component of the Stark-broadened line.

IV. APPROXIMATIONS FOR THE LINE CENTER AND THE WINGS

In the previous sections we developed a full impact formalism which took into account the electron impact contribution in addition to the turbulent quasistatic fields. As a result, complete profiles can now be obtained by appropriate β and γ averaging of Eqs. (3.29) and (3.30). The integrations must be carried out by numerical methods. However, in the remainder of this paper we shall not pursue this course. Rather at this stage we shall make an approximation which will allow us to proceed to an analytic derivation of line-profile formulas. This entails the assumption that the electron contribution can be neglected in the line wings. This assumption is undoubtedly well satisfied in many turbulent plasmas studied to date, where, as is discussed in Ref. 8, one finds that the quasistatic turbulent microfield is at least an order of magnitude greater than the classical thermal microfield. In such experiments as least, one can safely neglect the thermal quasistatic broadening due to the electrons, which, as is well known, is at most 50% of the thermal ionic contribution.

Therefore we are left with a quasistatic treatment in the Ly α wings, and thus we extend to anisotropic distributions [Eq. (2.4)] our previous isotropic calculations⁸ of the quasistatic profiles of the He I 4471-Å line. Note, however, that we still retain the impact electron broadening at and near the line center ($\alpha \approx 0$), where the unshifted central components are mainly influenced by such electron impacts.

The two complementary approximations just discussed are worked out below, yielding simple analytic formulas for the line profile. In a subsequent work, if it proves necessary, we shall improve our somewhat restricted treatment of the electron broadening in intermediate regimes by proceeding to a complete numerical analysis.

A. Line wings

We therefore introduce in Eqs. (3.29) and (3.30) the approximation

$$9\mathcal{G}[81\alpha^2 + (\alpha + \alpha_S)^2]^{-1} \approx \pi \delta(\alpha \pm \alpha_S) \text{ as } \mathcal{G} \rightarrow 0. \quad (4.1)$$

Observe that one proceeds to this limit without the need to invoke any wavelength-dependent criterion. Integration over the turbulent probability distribution of electric fields W then leads to an integral

of the form

$$\int_0^\infty d\beta \beta^2 e^{-\beta^2(a+b\gamma^2)} \delta\left(\alpha \pm \frac{3\beta\hbar\lambda_0^2}{2\pi m_e c}\right) = (\alpha/d)^2 \exp\{-[\alpha^2(a+b\gamma^2)/d^2]\}, \quad (4.2)$$

where

$$d = \frac{3}{2}\hbar\lambda_0^2/\pi m_e c, \quad a = E_0^2/\langle E_\perp^2 \rangle, \quad b = E_0^2/\eta^2 - 1/2\langle E_\parallel^2 \rangle.$$

We note that two distinct γ averages are to be considered, according to whether the anisotropy parameter $\eta^2 = 2\langle E_\parallel^2 \rangle/\langle E_\perp^2 \rangle$ is smaller or larger than unity.

$$1. \quad \eta^2 \equiv 2\langle E_\parallel^2 \rangle/\langle E_\perp^2 \rangle \leq 1$$

The corresponding γ quadratures are easily carried out with the aid of the following identities:

$$\int_0^1 d\gamma e^{-\alpha^2 b \gamma^2/d^2} = \frac{1}{2} \left(\frac{\pi}{2}\right)^{1/2} \frac{d}{\alpha} \Phi(\alpha\sqrt{b}/d), \quad (4.3)$$

$$\int_0^1 d\gamma \gamma^2 e^{-\alpha^2 b \gamma^2/d^2} = \frac{1}{2(\alpha^2 b/d^2)^{3/2}} \times \left(\frac{\sqrt{\pi}}{2} \Phi(\alpha\sqrt{b}/d) - \frac{\alpha}{d} \sqrt{b} e^{-\alpha^2 b/d^2}\right), \quad (4.4)$$

with Φ as the Fresnel error integral,

$$\int_{-1}^{+1} d\gamma \gamma^{0,2} e^{-\alpha^2(a+b\gamma^2)/d^2} = 2e^{-\alpha^2(a+b\gamma^2)/d^2} \times \begin{cases} \frac{1}{2}B(1, \frac{1}{2}) {}_1F_1(1; \frac{3}{2}; -\alpha^2 b/d^2), & \text{for } \gamma^0, \\ [-\frac{1}{2}B(\frac{1}{2}, 2) {}_1F_1(2; \frac{5}{2}; -\alpha^2 b/d^2) + \frac{1}{2}B(1, \frac{1}{2}) {}_1F_1(1; \frac{3}{2}; -\alpha^2 b/d^2)], & \text{for } \gamma^2, \end{cases} \quad (4.7)$$

where ${}_1F_1$ is a confluent hypergeometric function and B is the β function. These results lead to line profiles given by

$$S_\parallel(x) = \frac{2}{3}\pi Z x^2 e^{-x^2/f} {}_1F_1(2; \frac{5}{2}; -x^2), \quad (4.8)$$

$$S_\perp(x) = \frac{1}{3}\pi Z x^2 e^{-x^2/f} [3 {}_1F_1(1; \frac{3}{2}; -x^2) - {}_1F_1(2; \frac{5}{2}; -x^2)]. \quad (4.9)$$

Equations (4.5), (4.6), (4.8), and (4.9) represent our final results for the line profile of the turbulently broadened wings of the Lyman- α line. When the turbulence is isotropic, that is, when $\eta^2 = 1$, all four equations reduce, as expected, to a common result,

$$S_\parallel(y) = S_\perp(y) = \frac{4}{3}(\pi a)^{1/2} y^2 e^{-y^2}, \quad (4.10)$$

where

$$a = E_0^2/\langle E_\perp^2 \rangle, \quad y = (\alpha/d)a^{1/2} = \Delta\lambda(d\langle E_\perp^2 \rangle)^{1/2}.$$

$$\Phi(y) = \frac{2}{\pi^{1/2}} \int_0^y e^{-t^2} dt.$$

This leads to the following expressions for the line profiles:

$$S_\parallel(x) = \frac{1}{2}\pi Z e^{-x^2/f} [\pi^{1/2} x \Phi(x) - \pi^{1/2} \Phi(x)/2x + e^{-x^2}], \quad (4.5)$$

$$S_\perp(x) = \frac{1}{4}\pi Z e^{-x^2/f} [\pi^{1/2} x \Phi(x) + \pi^{1/2} \Phi(x)/2x - e^{-x^2}]. \quad (4.6)$$

Here x is the dimensionless wavelength variable,

$$x = \frac{\alpha b^{1/2}}{d} = \frac{\Delta\lambda}{d} \left| \frac{1}{2\langle E_\parallel^2 \rangle} - \frac{1}{\langle E_\perp^2 \rangle} \right|^{1/2},$$

and f and Z are constants defined

$$f = b/a = |(\langle E_\perp^2 \rangle/2\langle E_\parallel^2 \rangle) - 1|,$$

$$Z = \left(\frac{2}{\pi\langle E_\parallel^2 \rangle}\right)^{1/2} \frac{E_0^3}{b\langle E_\perp^2 \rangle} = \left(\frac{2}{\pi}\right)^{1/2} \frac{E_0}{\langle E_\parallel^2 \rangle^{1/2}} \left| \frac{1}{1 - \langle E_\perp^2 \rangle/2\langle E_\parallel^2 \rangle} \right|.$$

Recall that the foregoing results are applicable only when the anisotropy parameter $\eta^2 \leq 1$.

$$2. \quad \eta^2 \equiv 2\langle E_\parallel^2 \rangle/\langle E_\perp^2 \rangle \geq 1$$

The γ averages are obtained from

B. Line center

There is no analytic dichotomy between $\eta^2 < 1$ and $\eta^2 > 1$, provided the dimensionless parameters are given their appropriate values. The β average now becomes

$$\int_0^\infty d\beta \beta^2 e^{-\beta^2(a+b\gamma^2)} = \frac{\sqrt{\pi}}{4} \frac{1}{(a+b\gamma^2)^{3/2}}, \quad (4.11)$$

while the γ average is

$$\int_{-1}^{+1} \frac{d\gamma \gamma^{0,2}}{(a+b\gamma^2)^{3/2}} = \begin{cases} \frac{2}{b} \left(\frac{1}{a^{1/2}} - \frac{1}{(a+b)^{1/2}} \right), & \text{for } \gamma^0, \\ \frac{2}{b^2} \left((a+b)^{1/2} + \frac{a}{(a+b)^{1/2}} - 2a^{1/2} \right), & \text{for } \gamma^2. \end{cases} \quad (4.12)$$

The corresponding profiles are Lorentzian and the intensities S_\parallel and S_\perp for both $\eta^2 \leq 1$ and $\eta^2 \geq 1$ are

given by the following expressions for the unshifted central components:

$$S_{\parallel}(\alpha) = 2R \left(1 - \frac{1}{f} + \frac{(1+f)^{1/2}}{f^{3/2}} \ln[f^{1/2} + (1+f)^{1/2}] \right), \tag{4.13}$$

$$S_{\perp}(\alpha) = R \left(3 + \frac{1}{f} - \frac{(1+f)^{1/2}}{f^{3/2}} \ln[f^{1/2} + (1+f)^{1/2}] \right). \tag{4.14}$$

Here f is once again defined as

$$f = b/a = | \langle E_{\perp}^2 \rangle / 2 \langle E_{\parallel}^2 \rangle - 1 |,$$

and R denotes the Lorentzian profile whose form is

$$R = 9\alpha / (81\alpha^2 + \alpha^2). \tag{4.15}$$

The quantity 9α is the normalized electron collision frequency [Eq. (3.24)] and $\alpha = \Delta\lambda / E_0$, the normalized wavelength. For the case of isotropic turbulence, that is, in the limit as $\eta^2 \rightarrow 1$, $f \rightarrow 0$,

$$S_{\parallel}(\alpha) = S_{\perp}(\alpha) = \frac{9}{2}(9\alpha) / (81\alpha^2 + \alpha^2). \tag{4.16}$$

V. NUMERICAL RESULTS

The wing contributions to the full line profile are illustrated in Figs. 2(a) and 2(b). They were computed for the case for which the root-mean-square electric field of the turbulent fluctuations equaled 20 times the Holtzmark normal field E_0 , namely,

$$\langle E^2 \rangle^{1/2} = (\langle E_{\parallel}^2 \rangle + \langle E_{\perp}^2 \rangle)^{1/2} = 20E_0. \tag{5.1}$$

Figure 2(a) shows a plot of S_{\parallel} and S_{\perp} computed from Eqs. (4.5) and (4.6) for an anisotropy parameter of magnitude $\eta^2 = 0.1825$. Figure 2(b) shows the corresponding profiles calculated from Eqs. (4.8) and (4.9) for an anisotropy parameter equal to 9. With these choices of η^2 , the wavelength variable x plotted along the abscissa of both figures has identical values, namely,

$$x = \alpha b^{1/2} / d = 0.1106 \Delta\lambda / E_0 d. \tag{5.2}$$

This makes for easier comparison of the two figures, and the effects of the turbulence anisotropy are thereby more clearly brought out.

We see that the wing formulas (4.5), (4.6), (4.8), and (4.9) make no contribution at the exact line center $x = 0$. To obtain the complete profile also valid at and near $x = 0$, one must add to Figs. 2(a) and 2(b) the appropriate Lorentzian profiles given by Eqs. (4.13) and (4.14). For the parameters η^2 chosen above one then finds that at and near the line center

$$\begin{aligned} S_{\parallel}(\alpha) &= 2.292(9\alpha) / (81\alpha^2 + \alpha^2), \\ S_{\perp}(\alpha) &= 2.854(9\alpha) / (81\alpha^2 + \alpha^2), \end{aligned} \tag{5.3}$$

for $\eta^2 = 0.1825$, and

$$\begin{aligned} S_{\parallel}(\alpha) &= 2.506(9\alpha) / (81\alpha^2 + \alpha^2), \\ S_{\perp}(\alpha) &= 2.747(9\alpha) / (81\alpha^2 + \alpha^2), \end{aligned} \tag{5.4}$$

for $\eta^2 = 9.0$.

The effects of anisotropy in the turbulent micro-field on line shape are brought out more forcefully by plotting the ratio of S_{\parallel}/S_{\perp} as a function of the relevant quantities. Figure 3 shows such a plot obtained from the line-wing formulas (4.5), (4.6),

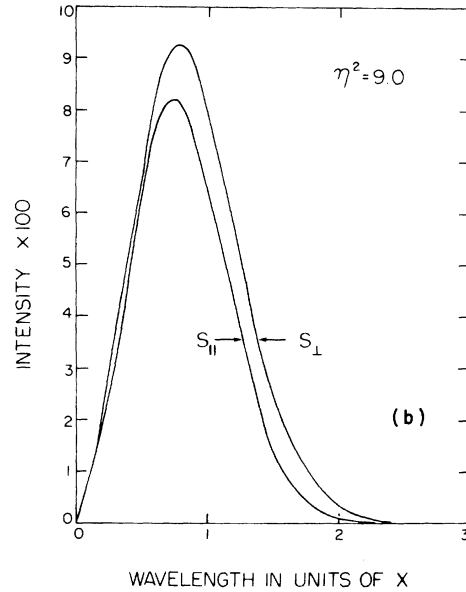
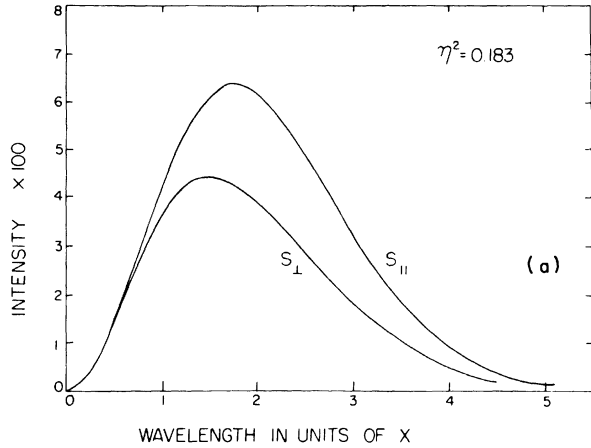


FIG. 2. (a) Wing contribution to the normalized line-intensity profile as calculated from Eqs. (4.5), (4.6), (4.8), and (4.9). S_{\parallel} is the intensity viewed along the axis of symmetry z , and S_{\perp} is the intensity perpendicular to it. The anisotropy parameter $\eta^2 = \langle 2E_{\parallel}^2 \rangle / \langle E_{\perp}^2 \rangle = 0.183$. To obtain the full line profile one must superpose contributions from the line center given by Eqs. (4.13) and (4.14). (b) Same as (a), except that the anisotropy parameter $\eta^2 = 9.0$.

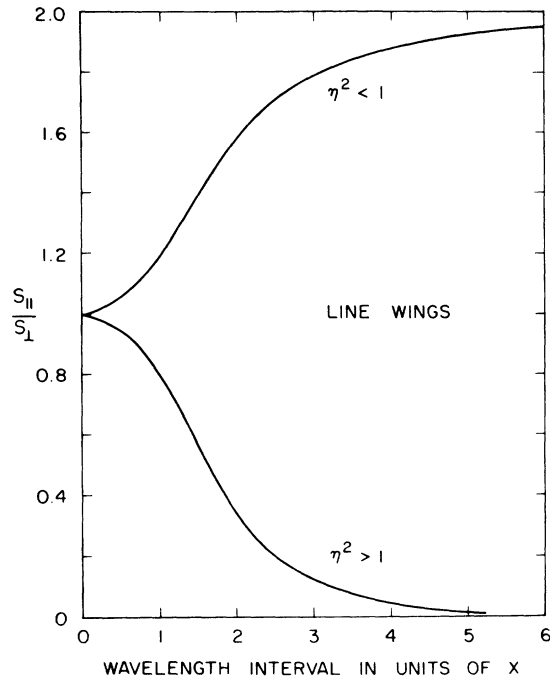


FIG. 3. Ratio of the intensities $S_{||}/S_{\perp}$ at the line wings as a function of the normalized wavelength parameter $x = \alpha b^{1/2}/d$ defined in the paragraph following Eq. (4.6).

(4.8), and (4.9). It is clear that for a given η^2 different portions of the line wings exhibit different values of the intensity ratio $S_{||}/S_{\perp}$. This suggests that careful measurements of the relative values of $S_{||}$ and S_{\perp} in a turbulent plasma may not only yield information about the absolute value of the turbulent electric field, but that one may also derive the degree of anisotropy η^2 of the field fluctuations.

In contrast to the line wings, where the ratio $S_{||}/S_{\perp}$ is a strong function of the wavelength x , the same ratio is independent of wavelength at and near the line center. This is obvious by taking the ratio of Eq. (4.13) and (4.14). A plot of this ratio as a function of η^2 is illustrated in Fig. 4. We see that as η^2 increases from zero, $S_{||}/S_{\perp}$ increases from a value of 0.6667, reaches unity at $\eta^2 = 1$, and then approaches asymptotically the value 0.9053 as $\eta^2 \rightarrow \infty$. By and large, the ratio $S_{||}/S_{\perp}$ at the line center is much less effected by the degree of anisotropy η^2 than are the line wings.

VI. DISCUSSION

We have presented what we believe to be the first comprehensive calculations of a line profile broadened by plasma turbulence. The hydrogen Lyman- α line was chosen not so much because of its value as a diagnostic tool but rather because of the basic simplicity afforded by this transition. The computations are entirely analytic and they serve in a

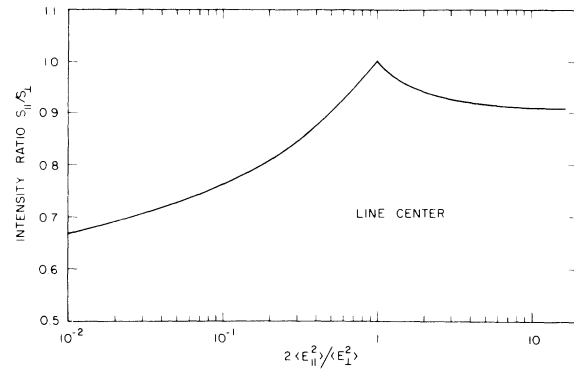


FIG. 4. Ratio of intensities $S_{||}/S_{\perp}$ at and near the line center, as a function of the anisotropy parameter $\eta^2 = 2\langle E_{||}^2 \rangle / \langle E_{\perp}^2 \rangle$. Note that at the line center this ratio is independent of the wavelength.

sense as “model” calculations for more complicated transitions. Such transitions include, for example, the higher-series hydrogen lines, where numerical procedures are unavoidable.

The limitations of the hydrogen Ly α line as a Stark-broadening diagnostic of conventional plasmas are well known. First, the line center is almost always strongly self-absorbed even when hydrogen is used in minute concentrations as a seed gas.¹³ Secondly, the Stark-broadening parameter is small, so that even if self-absorption were unimportant, a large part of the line profile may be strongly Doppler broadened.

However, matters can be very different in superdense plasmas such as those produced by focusing intense laser radiation on solid targets. Under such conditions hydrogenlike spectra (including the Ly α transition) of highly stripped heavy ions are observed. Plasmas with ion densities in excess of 10^{21} cm $^{-3}$ are being produced. If then the ion temperatures are not excessively high (below a few keV), Stark broadening prevails, as has been demonstrated in recent experiments.¹⁴

Our computations can be used for deducing the turbulent Ly α profiles of high- Z ions similar to those mentioned above. The turbulent microfield given by Eq. (2.4) is independent of the Z value and therefore the line wings remain unchanged. The Lorentzian line center $9\alpha/(81\alpha^2 + \alpha^2)$ changes because the collision parameter α of Eq. (3.24) changes: the line width $\Delta\lambda$ (in wavelength units) scales approximately as Z^{-2} , all other parameters (N, T) remaining constant. We stress, however, that the present calculations can be used for hot superdense plasmas only as long as the ion energies are sufficiently low so that the ion dynamics of the perturbers can be treated in the quasistatic approximation, as is implicitly assumed in this paper.

- *Work supported in part by the U. S. Energy Research and Development Administration Contract E(11-1)-3070.
- ¹C. F. Hooper, Jr., *Phys. Rev.* 165, 215 (1968).
- ²H. R. Griem and H. J. Kunze, *Phys. Rev. Lett.* 23, 1279 (1969).
- ³M. Raether and M. Yamada, *Phys. Lett.* 44A, 241 (1973).
- ⁴G. V. Sholin and E. A. Oks, *Dokl. Akad. Nauk SSSR* 209, 1318 (1973) [*Sov. Phys.-Doklady* 18, 254 (1973)].
- ⁵T. M. O'Neil, *Phys. Fluids* 17, 224 (1974).
- ⁶K. H. Spatschek, *Phys. Fluids* 17, 969 (1974).
- ⁷H. H. Klein and N. A. Krall, *Phys. Rev. A* 8, 881 (1973).
- ⁸G. Bekefi and C. Deutsch, *Comments Plasma Phys.* 2, 89 (1976); also, in *Quarterly Progress Report No. 111*, Research Laboratory of Electronics, MIT, 1973 (unpublished), p. 27.
- ⁹I. Alexeff, K. Estabrook, A. Hirose, W. D. Jones, R. V. Neidigh, J. N. Olsen, F. R. Scott, W. L. Stirling, M. M. Widner, and R. W. Wing, *Phys. Rev. Lett.* 25, 848 (1970).
- ¹⁰C. Deutsch, H. W. Drawin, L. Herman, N. Guyen-Hoe, and B. Petropoulos, Report CEA-R, 2913, Fontenay-aux-Roses, 1965 (unpublished); N. Guyen-Hoe, H. W. Drawin, and L. Herman, *J. Quant. Spectrosc. Radiat. Transfer* 7, 429 (1967).
- ¹¹C. Deutsch, *Phys. Rev. A* 2, 1258 (1970).
- ¹²H. R. Griem, A. C. Kolb, and K. Y. Shen, *Phys. Rev.* 116, 4 (1959).
- ¹³K. Behringer and W. R. Ott, in *Proceedings of the Eleventh International Conference on Phenomena in Ionized Gases*, Prague (unpublished), p. 396.
- ¹⁴A. M. Malvezzi, E. Jannitti, and G. Tondello, *Opt. Commun.* 13, 307 (1975).